2MTF I. THE TULLY-FISHER RELATION IN THE 2MASS J, H AND K-BANDS

Karen L. Masters[1], Christopher M. Springob[2,3], & John P. Huchra[1]

Draft version February 20, 2013

ABSTRACT

The 2 Micron All-Sky Survey (2MASS) Tully-Fisher Survey (2MTF) aims to measure Tully-Fisher (TF) distances to all bright inclined spirals in the 2MASS Redshift Survey (2MRS). Essential to this project is a universal calibration of the TF relation in the 2MASS J (1.2 μm), H (1.6 μm) and K (2.2 μm) bands. We present the first bias corrected or universal TF template in these bands. We find that the slope of the TF relation becomes steeper as the wavelength increases being close to $L \propto v^4$ in K-band and $L \propto v^{3.6}$ in J and H-bands. We also investigate the dependence on galaxy morphology showing that in all three bands the relation is steeper for later type spirals which also have a dimmer TF zeropoint than earlier type spirals. We correct the final relation to that for Sc galaxies. Finally we study the scatter from the TF relation fitting for a width dependent intrinsic scatter which is not found to vary significantly with wavelength.

Subject headings: galaxies: distances and redshifts — galaxies: clusters — galaxies: fundamental parameters — distance scale: infrared: galaxies

1. INTRODUCTION

The 2 Micron All-Sky Survey (2MASS) Tully-Fisher Survey (2MTF) is making use of existing high quality rotations widths, new HI widths and 2MASS photometry to measure Tully-Fisher (TF) distances for all bright inclined spirals in the 2MASS Redshift Survey (2MRS; Huchra *et al.* 2005). Previous peculiar velocity surveys have struggled to meet their potential because of large errors on individual measurements, poor statistics and uneven sky coverage. A survey based on 2MRS will provide both better statistics and greatly reduce the impact of the ZoA providing a *qualitatively* better sample for velocity–density field reconstructions. A significant amount of new HI observing (both at the Green Bank Telescope, and the Parkes Radio Telescope) has already been completed for the 2MTF project (Masters *et al.* in prep. see Masters 2007 for more details).

The first step in constructing the 2MTF catalog is to have a universal calibration of the TF relation in the 2MASS J, H and K-bands. As discussed in Masters *et al.* (2006; hereafter M06) the estimation of proper bias corrections for deriving TF templates is essential, not only if the template is to be used as a basis for unbiased distance estimates to galaxies with a wide range of rotational widths, but also if the template is to be used as a constraint in theories of galaxy formation. A bias corrected, or universal TF relation in the 2MASS J, H and K-bands does not currently exist. In this paper we provide such a TF template relation for use with 2MTF and in other applications. We also investigate the dependence of the NIR TF relation with wavelength and galaxy morphology and study the extent of the TF relation. Finally we measure the intrinsic scatter of galaxies

from the TF template relations as a function of galaxy rotation width. We finish by providing a recipe for deriving TF distances from data consisting of galaxy magnitudes, inclinations and rotational widths. We parameterize quantities dependent on the Hubble constant with $h = H_\circ/100$ km s^{-1} Mpc^{-1} where possible, and use $H_\circ = 74$ km s^{-1} Mpc^{-1} when we need to compare with $H_\circ$ independent measurements (*e.g.* calibrations of the TF zeropoint from primary distance measures).

2. THE 2MASS TF TEMPLATE SAMPLE

The 2MTF template sample discussed here originated in a cross-match of the 2MASS Extended Source Catalog (XSC) with all galaxies with rotation widths either from the Cornell HI digital archive (Springob *et al.* 2005), or from the database of optical rotation curves (ORCs) maintained by Martha Haynes and Riccardo Giovanelli at Cornell (see Catinella *et al.* 2005 for the most recent description of the ORCs). From this cross-match we pick galaxies in the vicinities of the 31 nearby clusters described in M06. In M06 the SFI++ sample (Springob *et al.* 2007) is used as a base for their related I-band TF template sample. This "SFI++ template sample" was comprised of galaxies which **in addition** to rotation widths from the above sources have I-band photometry as described in Haynes *et al.* 1999a. Using the same set of clusters as in M06 will ease comparisons between the I-band template from M06 and the J, H and K-band templates to be derived here. Using the terminology of M06 (and Giovanelli *et al.* 1997b; hereafter G97b) who describe an **in** sample in which all galaxies are clearly *bona fide* cluster members and a larger **in+** sample which may include galaxies merely in the vicinity of the cluster we consider mostly the **in+** sample for these clusters.

Roughly 70% of the SFI++ template sample (M06) are found in this "2MTF template sample". Some SFI++ galaxies are too low surface brightness in the NIR to be detected by 2MASS. This is especially a problem for the SFI++ since it was designed to be dominated by

Electronic address: kmasters@cfa.harvard.edu
[1] Harvard-Smithsonian Center for Astrophysics, 60 Garden Street, Cambridge, MA 02138
[2] Naval Research Laboratory, Remote Sensing Division Code 7213, 4555 Overlook Avenue, SW, Washington, D.C., 20375
[3] Department of Physics and Astronomy, Washington State University, Pullman, WA 99164

late type spirals which tend to have a lower NIR surface brightness. Of the final 2MTF template sample, 65% are also in the SFI++ template sample (the remaining 35% have available rotation widths, are present in the 2MASS XSC and located near one of the "template clusters", but do not have I-band photometry).

2.1. *Rotation Widths*

As described above, rotation widths are taken from the same source as the SFI++ template sample (M06), namely the HI digital archive published in Springob *et al.* (2005) supplemented by optical rotation curves (see *e.g.* Catinella *et al.* 2005). The correction from ORC to HI width (measured at 50% of the (peak$-rms$) on a fit to the sides of the profile) is described in M06 and is applied, with the modification that the optical radius (a_{83}, which is the radius contining 83% of the optical light) is estimated for galaxies which have only 2MASS photometry from the 2MASS parameter r_{ext} – the 2MASS XSC extrapolation or total radius. For galaxies with both 2MASS and I-band photometry we find $a_{83} = 0.56r_{ext}$, with a scatter of 13" – this is the relation used to calculate a_{83} for the 35% of the 2MTF sample which do not have available I-band photometry. The observed width must also be corrected for instrumental effects (Δ_s), inclination, cosmological broadening and the effect of turbulent motions (Δ_t) in the disk:

$$W_{corr} = \left[\frac{W_{F50} - \Delta_s}{1 + z} - \Delta_t \right] \frac{1}{\sin i}, \qquad (1)$$

We use $\Delta_t = 6.5$km s^{-1}. The instrumental correction will depend on the details of the telescope used: see Springob *et al.* (2005) for more information on this.

2.2. *Total Magnitudes and Inclinations*

The 2MASS XSC photometric quantities are described in great detail in Cutri *et al.* (2006). The quantities of interest here are the total magnitudes in the J, H and K bands (the extrapolated magnitudes are used), and the axial ratio. Inclinations are estimated from the deep I-band imaging taken as part of the SFI++ or SFI projects and described in Haynes *et al.* (1999a) for galaxies where this is available. In the 35% of galaxies for which no I-band imaging is available the J-band axial ratio (after correction for seeing as described in Masters, Giovanelli & Haynes 2003) is used to estimate the inclination. We choose the J-band over longer 2MASS bands (or the co-added image) in the hope that it best traces the inclination of the disk and is least affected by the bulge. We also use an intrisic axial ratio of 0.2 for all types of spirals to mitigate the effect of the bulge on the most edge-on galaxies. For all SFI++ galaxies in the 2MASS XSC (ie. not just galaxies used in this paper), an approximately one-to-one correlation is found between the I-band and J-band estimates of the inclination, with a rms scatter of $\sim 8.5°$. There is a slight tendency for the J-band axial ratio to imply the galaxy is less inclined than the I-band measurement, which is especially prominent for the most face-on (ie. lowest inclination) galaxies. We do not use any galaxies with J-band inclinations of less than 25° – galaxies with true inclinations this low would not make it into the SFI++ as they would not have been considered good candidates for TF distance measurement. There

is no significant trend of the difference between the two measures of inclination with galaxy morphological type. By looking at the scatter in the axial ratio measured in J-band vs. that measured in I-band we estimate that the error in the J-band axial ratio is $\sim \pm0.1$, remaining approximately flat with decreasing ellipticity. This is the error we carry forward into the error on the rotation widths for galaxies in which J-band inclinations are used. By comparison the I-band axial ratio has a mean reported error of ±0.04, increasing to ±0.06 for the most face-on galaxies, and decreasing to less than ±0.02 for the most inclined. The use of J-band axial ratios for 35% of the sample will obviously add some scatter into the final TF template.

Galactic extinction is estimated using the DIRBE dust map (Schlegel, Finkbeiner & Davis 1998), while dust extinction internal to the galaxies themselves is estimated using the luminosity dependent empirical relations found in Masters *et al.* (2003). A small K-correction is applied, also as described in Masters *et al.* (2003).

3. CONSTRUCTING A GLOBAL TEMPLATE

Many schools of thought exist on the best way to construct a TF template. In one method no attempt is made to correct for observational biases (*e.g.* Pizagno et al. 2007). The argument is that such corrections depend on various assumptions and so add an unmeasurable source of error into the template. Such templates must not be considered global in any sense and can only be compared to theory when mock catalogs with the same selection criteria are constructed. They also have the distinct disadvantage of introducing obvious biases into distances derived from TF. Another method (*e.g.* Theureau et al. 2007) attempts to construct an "unbiased" sample of galaxies so that no corrections are necessary – this has the disadvantage of requiring a large part of the data be rejected from the template sample, and because the rejected galaxies lie preferentially at the low mass end of the relation this will also result in a TF template relation which is not completely universal since it will be fit only to the most massive spirals. It is possible to construct a bias corrected or universal TF template in which observational sample biases are corrected using reasonable assumptions about the properties of the parent galaxy population. With the right assumptions this method is the only one which produces a *universal* or *global* TF relation which can be compared directly to theory and used without concern to derive TF distances. This is the approach we will take here.

A detailed description of all the relevant bias corrections which need to be applied to derive a universal TF relation has recently been published in M06; we refer the reader to that paper for more details. Both in M06 and this paper, the method used is based on that described in G97b. What follows is a list of all bias corrections, including details of how they have been modified to apply to 2MASS photometry and the template sample discussed here.

These corrections are applied *after* the magnitudes have been corrected for Galactic and internal extinction and the inclinations have been corrected for seeing; and after the HI widths have been corrected for instrumental broadening, the ORC widths corrected to the HI scale, and all widths have been corrected for inclination and

cosmological broadening.

1. *Incompleteness bias correction:* In any given cluster we preferentially observe galaxies which are scattered above the TF slope (because they are brighter and therefore more likely to make it into the sample). This has the result of shallowing the TF slope, brightening the zero point and reducing the measured scatter. The correction we apply for this effect is derived following the method described in G97b and M06. It is derived from Monte Carlo simulations of the difference between the expected and observed magnitudes requiring an input TF relation, TF scatter and spiral LF (which is used to estimate the completeness of the sample). We do the calculation only once, using as an input the TF relations and scatter uncorrected for this effect (but already corrected for the morphological dependence as described in #5 below). We discuss below the impact of these assumptions on the size of the bias correction.

A luminosity function was calculated for late-type galaxies ($T \geq 0$) in K-band by Kochanek et al. (2001). This LF includes S0/a galaxies ($T = 0$) as well as later types, but they found that the LF parameters were insensitive to moving the boundary to include only Sa and later galaxies. They fit a Schechter function with $M_{K*} - 5\log h = -22.98 \pm 0.06$ mags and $\alpha = -0.92 \pm 0.10$. This is the luminosity function we use to calculate the incompleteness of the template sample. To each measure incompleteness for a cluster we fit a function of the form

$$c(y) = \frac{1}{e^{(y-y_F)/\eta} + 1} \qquad (2)$$

The parameters of the fit to the K-band incompleteness function for each individual cluster sub-sample are given in Table 1. To convert the completeness to J and H bands we use a constant color estimates of $J - K = 1.04$ and $H - K = 0.28$ which are the average for all galaxies in the template sample. There are no large trends of $H - K$ color with absolute magnitude and only a slight trend for $J - K$ color to be smaller for dimmer galaxies (which could result in a very slight over-estimation of the incompleteness in J-band for the least luminous galaxies). This $J-K$ color is a little redder than that measured for a complete sample of 2MASS galaxies (Huchra *et al.* in prep.) although the $H - K$ color is consistent. Galaxies in the template sample are larger and more inclined that the average galaxy in 2MASS so even though this color is corrected for internal extinction as described in Masters *et al.* (2003) we expect them to be a little redder than average because this mean correction may still be a underestimate for the brightest most edge-on galaxies.

We use a bivariate fit to the full sample as our estimate of the universal TF relation. We do one round of the iteration – we use to calculate the bias corrections the initial relations (not corrected for incompleteness bias, but after the morphological correction discussed below is applied) which are

$$M_K - 5\log h = -22.228 - 8.919(\log W - 2.5),$$
$$M_H - 5\log h = -21.954 - 8.289(\log W - 2.5),$$
$$M_J - 5\log h = -21.198 - 8.030(\log W - 2.5).$$

This can be compared with the final output in Table 2. The slopes here are shallower than the final relation by ~ 1 mag/dex in K- and J-bands and 0.7 mag/dex in H-band. The zeropoints are brighter by ~ 0.2 mag in K- and J-bands and 0.1 mag in H-band. As shown in G97b and Masters (2005) changing the zeropoint and slope of the assumed UTF by these amounts will not change the magnitude of the derived bias correction significantly.

The assumed scatter we use is also the scatter from the initial relation (uncorrected for incompleteness bias but after correction for morphology) of

$$\epsilon_{\text{int,K}} = 0.41 - 1.43(\log W - 2.5),$$
$$\epsilon_{\text{int,H}} = 0.43 - 1.26(\log W - 2.5),$$
$$\epsilon_{\text{int,J}} = 0.45 - 1.08(\log W - 2.5),$$

(see Section 4 for an explanation of the derivation of this and the final output values). It is this assumption which has the biggest effect on the magnitude of the calculated bias correction. However, the scatter from the final TF relation is only 0.05 mag smaller than this value (in all 3 bands), and this is not enough of a difference to significantly change the derived corrected for the incompleteness bias (as shown in G97b and Masters 2005).

The magnitude of the bias correction for a given galaxy depends on a combination of the absolute magnitude of the galaxy and the distance to the cluster in which the galaxy is located (in the nearer clusters the sample is obviously complete to a fainter absolute magnitude limit). In G97b and M06 the bias correction is shown separately for galaxies in each of the clusters used in the template. Here we instead show bias corrections for all galaxies in all clusters together (Figure 1).

2. *Mean distances to cluster.* This small fixed bias for all galaxies in a given cluster arises from the fact that the log of the average of the distance is not equal to the average of the log of the distance (which is what we implicitly fit for when using magnitudes). This bias is easy to calculate once a line of sight depth for each cluster has been estimated. We use as a size estimate 1 Abell radius for the **in** sample, 2 Abell radii for **in+**. This bias is almost always much less than 0.1 mag, and is given for each cluster in Table 1 (β_{size}).

3. *Cluster size – incompleteness.* In a given cluster we preferentially observe dimmer galaxies only in the closest parts of the cluster - creating a small bias in the observed magnitudes which is easily corrected for using the completeness we have already calculated for each cluster and assumptions about the size of the cluster. This bias is very small (less than 0.1 mags) for most galaxies in the sample.
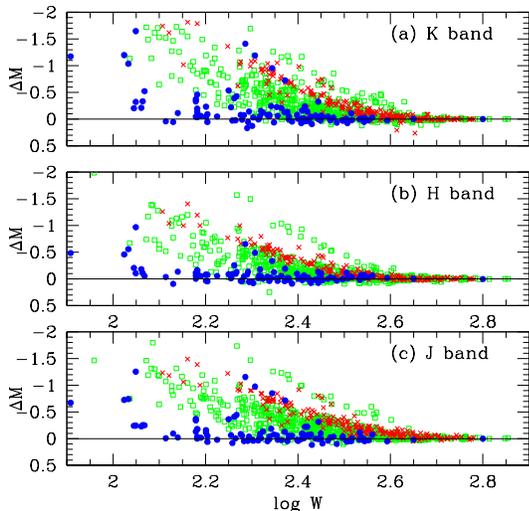
FIG. 1.— Incompleteness bias corrections in J, H and K-bands for all galaxies. Points are coded by the redshift of the cluster the galaxy belongs to. Blue dots: $v_{\rm cluster} < 3000$ km s^{-1}; green squares: 3000 km s$^{-1} < v_{\rm cluster} < 7000$ km s^{-1}; red crosses: $v_{\rm cluster} > 7000$ km s^{-1}. This illustrates how the size of the bias correction for a given galaxy depends both on the luminosity of the galaxy and the completeness of the individual cluster sub-sample the galaxy belongs to. It also illustrates that clusters at similar redshifts but in different parts of the sky have quite different levels of completeness.

4. *Edge of catalog bias and Malmquist bias.* Following G97b and M06 we argue that both of these biases are negligible in the sample and therefore make no correction for them.

5. *Morphological correction:* We observe that the slope for earlier type spirals is shallower than for later types and that they have a brighter zeropoint. We correct to an "Sc" (type $T = 5$) relation in K-band using,

$$\begin{aligned}\Delta M_{\rm Sa} &= 0.19 - 3.16(\log W - 2.5): & T \leq 2\\ \Delta M_{\rm Sb} &= 0.01 - 1.46(\log W - 2.5): & 3 \leq T \leq 4\end{aligned}$$

In H-band we use,

$$\begin{aligned}\Delta M_{\rm Sa} &= 0.21 - 2.92(\log W - 2.5): & T \leq 2\\ \Delta M_{\rm Sb} &= 0.01 - 1.26(\log W - 2.5): & 3 \leq T \leq 4.\end{aligned}$$

In J-band we use,

$$\begin{aligned}\Delta M_{\rm Sa} &= 0.23 - 2.86(\log W - 2.5): & T \leq 2\\ \Delta M_{\rm Sb} &= 0.02 - 1.31(\log W - 2.5): & 3 \leq T \leq 4.\end{aligned}$$

These values are as measured using the data for each sub-sample (separated by morphological type) **before** it has been corrected for sample incompleteness bias (above) . The final fits to the sample separated by morphological type once the incompleteness bias correction has been applied are listed in Table 2, and shown for K-band in Figure 4. They are very similar to what is used here.

The variation of the TF relations with morphological type is found to have a similar magnitude in all 3 bands, and a similar dependence on the rotational width. The morphological dependence of the TF relation is discussed further in Section 3.2.

The caveat to be added here is that if the incompleteness for earlier type spirals is greater than for the later types, then this variation in the TF relation may not be physical but rather the impact of an underestimate of the incompleteness correction for earlier type spirals. Naively, in the NIR we expect the selection criteria to be worse for late types, however our selection function also takes into account the availability of rotation width data which selects against earlier types spirals. Without a reliable luminosity function (LF) separated by morphological types along the spiral sequence there is no way to tell if the change in slope is due to incompleteness, or telling us something physical about the different types of spirals. There is also a possibility that it is related to variations in the amount of internal extinction in different types of spirals as a function of their intrinsic size, although that effect is not large in the NIR (Masters *et al.* 2003). In any case the difference in the relations between spiral types should be corrected for to construct the final "universal" TF relation for Scs.

6. *Cluster peculiar velocity.* To combine all the individual cluster samples into a global TF relation, a peculiar velocity must be estimated for each cluster. We use the peculiar velocities derived in M06 which considered the same set of clusters as is used here. For more details on this step we refer the reader to M06. Below we discuss further the impact this has on the zeropoint of the TF relation, and possible error introduced into the zeropoint by using a subset of the most distant clusters to define a zero-point rest frame.

The global template TF relation is shown in Figure 2 for the **in+** samples in all three bands. A summary of linear fits (direct, inverse and bivariate respectively considering errors in the magnitude direction, width direction and in both directions) to various subsets of the **in+** sample is given in Table 2. In that table zeropoints (labeled a) are reported for $H_{\rm o} = 100$ km s^{-1} Mpc^{-1}. The slopes are labeled, b. The last four columns of Table 2 list the error on the bivariate zeropoint and slope, and the standard deviation and absolute deviation of the points from the bivariate relation. We list results for three fitting methods to aid comparisons with other results (*e.g.* Section 3), but our preferred method is the bivariate fit which considers errors in both the magnitude and rotational width. Direct fits consider errors only in the magnitude and are the most affected by magnitude incompleteness in the sample. It is often suggested that using inverse fits completely removes the effects of incompleteness bias - however since inclination dependent corrections for both the magnitudes and widths create implicit cross-dependences in the final quantities there will be some incompleteness bias still present in the inverse fits. Our preferred result (using the bivariate fit and all corrections described above) for the TF relation is then:

$$\begin{aligned}M_K - 5\log h &= -22.030 - 10.017(\log W - 2.5),\\ M_H - 5\log h &= -21.833 - 9.016(\log W - 2.5),\\ M_J - 5\log h &= -20.999 - 9.070(\log W - 2.5).\end{aligned}$$

TABLE 1
K-band Incompleteness Function Co-efficients and Cluster Size Bias.

Cluster Name	Redshift km s^{-1}	N_{in}	N_{in+}	y_F mags	η	σ_d/d	in β_{size} mags	in+ β_{size} mags
N383	4865	14	42	-21.03	1.01	0.03	-0.002	-0.010
N507	4808	17	28	-21.87	0.42	0.03	-0.002	-0.010
A262	4665	28	65	-22.56	0.69	0.03	-0.003	-0.010
A397	9594	13	13	-23.19	0.49	0.02	-0.001	-0.001
A400	6934	27	89	-23.03	0.61	0.02	-0.001	-0.005
A569	6011	13	15	-20.43	0.38	0.02	-0.001	-0.006
A634	7922	6	6	-21.65	0.49	0.02	-0.001	-0.001
Cancer	4939	22	75	-21.88	0.66	0.03	-0.002	-0.009
A779	7211	13	19	-22.85	0.47	0.02	-0.001	-0.004
A1314	9970	6	6	-20.70	0.05	0.02	-0.001	-0.001
A1367	6735	37	54	-23.41	0.62	0.02	-0.001	-0.005
Ursa Major	1101	16	25	-17.26	1.24	0.14	-0.046	-0.186
Coma	7185	36	52	-22.59	0.42	0.02	-0.001	-0.004
A2199/7	8996	8	25	-23.18	0.43	0.02	-0.001	-0.003
Pegasus	3519	20	39	-19.73	0.12	0.04	-0.005	-0.018
A2634	8895	18	35	-22.48	0.41	0.02	-0.001	-0.003
A2806	7867	9	9	-23.07	0.31	0.02	-0.001	-0.001
A2877	6974	7	7	-21.51	0.36	0.02	-0.001	-0.001
A194	5036	24	32	-21.24	1.14	0.03	-0.002	-0.009
Eridanus	1536	18	27	-18.78	0.53	0.10	-0.024	-0.095
Fornax	1321	11	23	-17.58	0.43	0.11	-0.032	-0.129
A496	9809	4	4	-22.66	0.80	0.02	-0.001	-0.001
Antlia	3120	12	29	-21.61	0.18	0.05	-0.006	-0.023
Hydra	4075	23	32	-21.61	0.45	0.04	-0.003	-0.014
NGC 3557	3120	5	11	-21.79	0.62	0.05	-0.005	-0.020
Cen 30	3322	20	33	-21.37	0.80	0.05	-0.005	-0.020
ESO 508	3196	7	15	-21.88	0.65	0.05	-0.006	-0.022
A3574	4817	10	25	-22.40	0.77	0.03	-0.002	-0.010
Pavo II	4444	7	24	-23.92	0.31	0.03	-0.003	-0.011
Pavo I	4055	6	14	-21.06	0.21	0.04	-0.003	-0.014
MDL59	2317	7	15	-20.06	0.39	0.07	-0.010	-0.042

NOTE. — Column(1) - cluster name ordered by RA in the North (top half) and South (bottom half). Column(2) - cluster redshift in the CMB frame. Columns (3) & (4) - number of galaxies in **in** and **in+** samples respectively. Columns (4) & (5) - parameters of the incompleteness function for the cluster (Equation 2). Column (6) - estimate of size σ_d, divided by an estimate of the distance, $d = v_{cmb}/H_\circ$, for each cluster. Columns (7) & (8) - cluster size–incompleteness bias for the **in** and **in+** samples respectively.

In the fits both the observational errors and an estimate of the intrinsic error of the TF relation are used to weight points. We do not fit for the intrinsic scatter as the same time as the slope and zero-point, but measure it after and iterate the fit and scatter measurement until convergence is reached.

The zeropoint derived for the TF relation from the "basket of clusters" method comes from an assumption that the net motion of a subset of the most distant clusters is zero in the CMB frame (the so-called "cluster reference frame"). We use in this paper the same zeropoint calibration (in terms of the peculiar velocities of the clusters in the CMB frame) that was derived in M06 for the I-band TF relation. This zeropoint could have a systematic offset from the true zeropoint if there is a net motion of the cluster reference frame with respect to the CMB. The expected size of this possible offset was estimated in M06 under the assumption that the peculiar velocities of clusters are characterized by an rms 1D velocity dispersion with $\sigma_v = 298 \pm 34$km s^{-1} (as measured in M06). They use this dispersion to estimate the possible offset from the random peculiar velocities of clusters to be $|\Delta M| \sim 0.03$ mag. This would be an underestimate of the zeropoint offset if there were coherent peculiar motions on the scale of the entire cluster sample. However as the sample extends to a distance of $cz = 10000$ km s^{-1} and clusters are located all over the sky a large

effect from coherent peculiar velocities seems unlikely. In M06 a Cepheid calibration of the I-band TF relation was compared to the "basket of clusters" zeropoint and agreement is found for a Hubble constant of $H_\circ = 74 \pm 2$ (random) ± 6 (systematic) km s^{-1} Mpc^{-1}. The fact that this is identical to $H_\circ = 74 \pm 2$ km s^{-1} Mpc^{-1} found by Sánchez *et al.* (2006) from a combination of WMAP and the 2dF galaxy redshift survey suggests that the "basket of clusters" zeropoint is not biased significantly by any bulk flows across the sample.

3.1. Wavelength Dependence

As found by numerous other authors (see Section 5 below for a discussion of some recent results in the NIR) the TF relation steepens as the wavelength of the band it is measured in increases. We find no significant evidence for wavelength dependence of the scatter (see Section 4 below). Figure 3 summarizes the trends of the slope and zeropoint with wavelength including both the relations reported in this paper for J, H and K-bands as well as the I-band result from the related sample of M06.

We find that the slope of the TF relation is very close to the simple theoretical expectation of $b = -10$ ($L \propto v^4$) in K-band, with $L_K \propto v^{4.00\pm0.04}$. In H-band we find $L_H \propto v^{3.61\pm0.04}$ and in J-band we find $L_J \propto v^{3.63\pm0.05}$. For their related sample, and using the same method as in this paper M06 find that in I-band $L_I \propto v^{3.14\pm0.04}$.

TABLE 2
TF PARAMETERS

Sample	N	Direct fit		Inverse fit		Bivariate fit					
		a_{dir}	b_{dir}	a_{inv}	b_{inv}	a_{bi}	b_{bi}	ϵ_a	ϵ_b	$\sigma_{\rm SD}$	$\sigma_{\rm abs}$
K-band											
No corrections											
Full	888	-22.271	-6.548	-22.261	-10.032	-22.215	-7.254	0.019	0.110	0.571	0.401
Morphological correction only											
Full	888	-22.312	-7.932	-22.250	-10.005	-22.228	-8.919	0.017	0.102	0.510	0.349
Bias correction only											
Sa	101	-22.461	-5.473	-22.297	-7.565	-22.143	-6.954	0.048	0.239	0.463	0.337
Sb	345	-22.132	-7.205	-22.227	-9.417	-22.034	-8.635	0.025	0.165	0.513	0.353
Sc	442	-22.031	-8.329	-22.409	-11.530	-22.039	-10.092	0.022	0.175	0.579	0.427
Full	888	-22.094	-7.296	-22.252	-10.011	-21.997	-8.647	0.015	0.093	0.551	0.398
All corrections											
Full	888	-22.107	-8.849	-22.244	-9.996	-22.030	-10.017	0.015	0.098	0.523	0.372
Low mass	303	-21.831	-8.280								
High mass	374	-22.281	-8.058								
H-band											
No corrections											
Full	888	-21.990	-6.438	-21.981	-9.595	-21.943	-7.068	0.019	0.117	0.580	0.414
Morphological correction only											
Full	888	-22.012	-7.608	-21.972	-9.580	-21.954	-8.289	0.018	0.114	0.542	0.382
Bias correction only											
Sa	101	-22.196	-5.383	-22.004	-7.429	-21.996	-6.084	0.054	0.265	0.475	0.355
Sb	345	-21.910	-6.833	-21.954	-9.100	-21.842	-7.803	0.027	0.165	0.526	0.365
Sc	442	-21.838	-7.807	-22.119	-10.976	-21.847	-9.165	0.024	0.189	0.569	0.423
Full	888	-21.879	-7.001	-21.975	-9.587	-21.812	-7.896	0.016	0.105	0.553	0.401
All corrections											
Full	888	-21.893	-8.235	-21.967	-9.575	-21.833	-9.016	0.016	0.106	0.530	0.382
Low mass	303	-21.612	-6.993								
High mass	374	-21.972	-7.838								
J-band											
No corrections											
Full	888	-21.236	-6.343	-21.218	-9.448	-21.192	-6.905	0.020	0.133	0.613	0.446
Morphological correction only											
Full	888	-21.252	-7.433	-21.208	-9.427	-21.198	-8.030	0.019	0.120	0.587	0.423
Bias correction only											
Sa	101	-21.349	-5.604	-21.234	-7.347	-21.218	-6.093	0.056	0.297	0.494	0.363
Sb	345	-21.064	-7.084	-21.188	-8.914	-21.016	-7.795	0.027	0.185	0.562	0.404
Sc	442	-21.021	-8.244	-21.352	-10.831	-21.017	-9.228	0.026	0.202	0.625	0.476
Full	888	-21.037	-7.408	-21.207	-9.425	-20.985	-8.104	0.017	0.117	0.597	0.444
All corrections											
Full	888	-21.050	-8.428	-21.199	-9.411	-20.999	-9.070	0.017	0.116	0.578	0.426
Low mass	303	-20.695	-6.588								
High mass	374	-21.086	-8.289								

NOTE. — Column (1) describes the sample used to fit to, column (2) shows the total number of galaxies in that sample. Columns (3-8) show parameters for $M - 5 \log h = a + b(\log W - 2.5)$ using direct, inverse and bivariate fits. Also shown for the bivariate fits are the error on a and b (columns 9 & 10), and the scatter calculated as the standard deviation (column 11) and absolute deviation (column 12). Inverse and bivariate fits are not reported for the sample divided by galaxy size since the artificial $\log W$ cut-off which is applied creates a large bias in those fits.
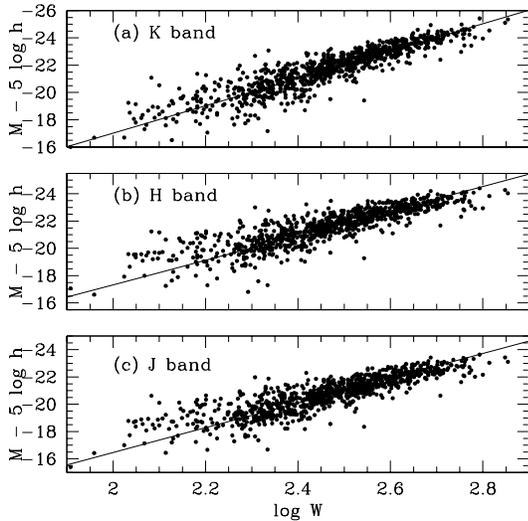
FIG. 2.— Global TF relation for (a) K-band, (b) H-band (c) J-band(**in+** sample). The solid line is all panels shows the respective bivariate fit to the data (see Table 2).
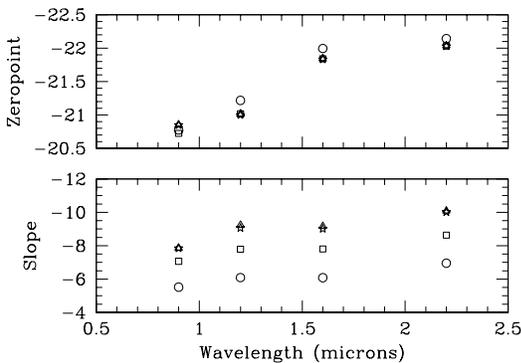

FIG. 3.— Trends of the (a) zeropoint and (b) slope of the TF relation with wavelength. I-band results from the related sample of M06. Circles shows the result for Sas, squares for Sbs, triangles for Scs and stars for the combined sample (with magnitudes of Sas and Sbs corrected to fall on the Sc relation).

The zeropoint of the TF relation also changes with band. This change as expected is consistent with the average colors found for galaxies in the template sample of $J - K = 1.04$ and $H - K = 0.28$, with $a_J - a_K = 1.03$ and $a_H - a_K = 0.20$.

3.2. *Morphological Dependence*

We find in all three 2MASS bands that the slope of the TF relation steepens as the sample changes from earlier type to later type spirals (see Figures 3 and 4). This is also as found in I-band for the related SFI++ template sample (M06). The amount the slope changes appears to be relatively independent of the band of the TF relation magnitudes. We find little evidence for a zeropoint change between Sb and Sc galaxies, but Sa's do appear to have a zeropoint ~ 0.2 mags brighter than later type spirals in all three 2MASS bands.

These findings are contrary to the commonly held idea that morphological variation of the TF relation disappear almost completely in the NIR (*e.g.* Noordermeer & Verheijin 2007). This conclusion was based on a lack of
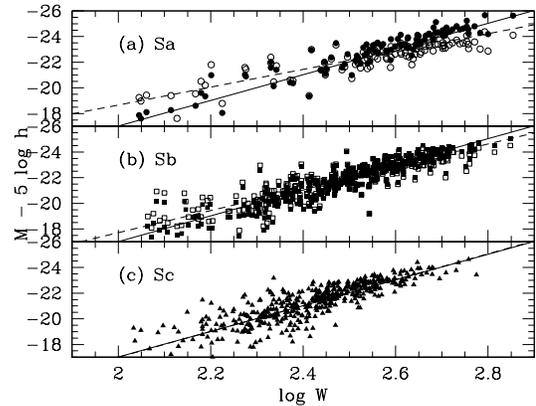

FIG. 4.— K-band TF relation for the **in+** sample separated by morphological type (a) Sa and earlier; (b) Sb; (c) Sc and later. In each panel open symbols show the magnitudes corrected for all biases except morphological type. The dashed lines show the fits to these points. The filled symbols are the magnitudes after the morphological type correction is applied and the solid line in all panels shows the final fit to the full sample.

morphological dependence found by Aaronson & Mould (1983) and Peletier & Willner (1993) in the H-band TF relation, and was used to argue that the morphological dependence seen in the bluer bands could be attributed to differences in star formation history between types of spirals. The clear (if small) morphological dependence we pick up is presumably a result of our much larger sample size, and indicates that the change in the TF relation cannot be totally accounted for by the details of star formation history and instead may be related either to something more fundamental about the dynamics of disk galaxies along the Hubble sequence, or possibly to the dust content or metallicity of different types of spiral galaxies (although dust content is not seen to have a large impact in the NIR, Masters *et al.* 2003). In M06 we interpreted the change in slope between different types of spirals (if real and not an effect of varying incompleteness for different spiral types) as possibly being due to the dark matter halos of earlier type spirals being less concentrated at a given rotation velocity than later types. The large caveat here is that if the incompleteness bias is significantly larger for Sas than later type spirals, the slope of the Sa relation may be artificially shallowed and the zeropoint artificially brightened by the effects of this bias. Naively, in the NIR we expect the selection criteria to be worse for late types, however our selection function also takes into account the availability of rotation width data which selects against earlier types spirals, so either could be true. However it should also be noted that much of the change in slope is driven by massive Sa's (and Sb's) which should be unaffected by the incompleteness bias.

3.3. *Luminosity Dependence*

There is present in Figure 2 a hint that both at the very high mass and very low mass ends of the TF relation galaxies turn off slightly from the mean trend. We divide the full sample into "luminosity classes" to study this further using $\log W$ limits of $\log W < 2.4$; $\log W > 2.5$ which roughly selects the lowest and highest mass thirds of the sample. We fit the TF relation to these subsets; the results are in Table 2. In this case we are adding in an artificial strict rotation width limit so biasing both

the inverse and bivariate fits. We therefore report only the direct fit in Table 2. We see evidence that at both the high and low mass ends of the relation there is a slightly shallower slope, however in both cases and in all 3 bands this difference is very small.

Disentangling fully the luminosity dependence of the slope and the morphological dependence will be difficult since as illustrated in Figure 4 the $\log W$ distribution of the different types of spirals is quite different with many more high mass Sas compared to Scs. We note here that we look for luminosity dependence after correcting for morphological type as described in Section 3. Searching for a variation is also complicated by the impact of the incompleteness bias correction. We assume a linear TF relation to calculate the bias, which has a large effect at the low mass end of the relation. Separating a variation of the TF at the low mass from this incompleteness bias is obviously not trivial.

There have been several studies in the optical passbands of the low mass end of the TF relation including Kannappan, Fabricant & Franx (2002) who describe a split in the dwarf extension of the TF relation in U, B and R-bands confirming findings by Pierini (1999) in the B-band. Hints of a deviation can also be seen in the I-band TF presented in M06. Typically the deviation has been seen to make the slope of the linear relation steeper for low mass galaxies, while here we see hints of it shallowing. However in other studies (which may have been more complete for low mass galaxies) there was no correction for incompleteness bias, which is found to be quite large in our sample. The bias correction we apply brightens all points at $\log W < 2.4$ by up to a magnitude or more (see Figure 1), so any conclusions we draw on the low mass end of the relation are highly dependent on the assumption which went into the bias correction. The choice of rotation width measure and turbulent motion corrections applied to the widths also impact the small rotation width galaxies much more greatly. We use rotation widths based on the width of the HI line at 50% of the peak, and corrected for a turbulent motion using a linear correction of 6.5 km s^{-1} as justified in Springob *et al.* (2005).

At the high mass end of the TF relation, Noordermeer & Verheijen (2007) recently argue that very massive galaxies lie systematically to the right of the mean K-band TF relation. This the same as the trend we see here and which is also present in the I-band relation of M06.

4. THE SCATTER IN THE TF RELATION

The scatter in the TF relation is important, both to understand the errors on distances derived from TF, and as a constraint for models of galaxy formation. As in G97b and M06 we observe that the scatter in the TF relation increases with decreasing rotation width. We therefore parametrize the scatter as

$$\sigma = a + b(\log W - 2.5). \qquad (3)$$

In both G97b and M06 there is a discussion of the effect incompleteness bias can have on the observed scatter. We find that in this sample the bias on the scatter is fairly small, so we neglect to correct for it. It should then be noted that the scatters quoted here are underestimates of the real scatter by something on the order of 10%

at the low mass end of the relation. At the high mass end (above $\log W \sim 2.5$ or $W \sim 320$ km s^{-1}) there is no longer any impact from incompleteness bias on the scatter.

The measured scatter (standard deviation) is shown for all 3 2MASS bands in Figure 5. A linear fit to the total scatter gives

$$\epsilon_{\mathrm{obs,K}} = 0.54 - 0.87(\log W - 2.5)$$
$$\epsilon_{\mathrm{obs,H}} = 0.54 - 0.89(\log W - 2.5)$$
$$\epsilon_{\mathrm{obs,J}} = 0.56 - 0.66(\log W - 2.5)$$

(shown by the dash-dot lines in the figure). We estimate the total measurement errors from the template sample as a function of rotation width. These values are shown by the dotted lines in Figure 5. The lower line at $\sigma \sim 0.1$ shows the measurement error on the total magnitudes (in the respective bands) which at all widths is the least important source of error. The middle line shows a value of $|b|\sigma_W$ which is the error on the measured rotation widths expressed in magnitudes. Adding these two contributions in quadrature approximates the total measurement error (this neglects the covariances between the two values which arise from the inclination corrections). Using this estimate of the total measurement error we also fit for an intrinsic scatter which varies with rotational width finding:

$$\epsilon_{\mathrm{int,K}} = 0.35 - 1.17(\log W - 2.5)$$
$$\epsilon_{\mathrm{int,H}} = 0.38 - 1.14(\log W - 2.5)$$
$$\epsilon_{\mathrm{int,J}} = 0.39 - 0.78(\log W - 2.5)$$

These estimates of the intrinsic scatter in the TF relation are shown by the dashed line in Figure 5; the solid line shows the quadrature sum of this and the total measurement error. This sum provides a better fit to the observed errors than the straight line fit.

There is no significant evidence for a variation of the TF scatter with band, however there is a consistent increase in the zeropoint and decrease in the variation with $\log W$ from K- to J-band. We also find a larger total scatter than in the I-band sample of M06 (which reports $\epsilon_{\mathrm{int,I}} = 0.35 - 0.37(\log W - 2.5)$) but this may be related to the larger errors on correcting the widths for inclination by using 2MASS axial ratios. This may not be totally accounted for in our estimate of the total measurement error and certainly could add significant covariance between the magnitude and width errors, so a direct comparison between the scatter measured here and that of M06 should be done carefully.

In the sub-samples divided by morphological type we have not fit separately for the intrinsic scatter a a function of $\log W$. From Table 2 however we can compare the total scatter of the different subsets from their own TF relations. We find in all three bands a consistent increase of the total scatter from Sa to Sc galaxies. However disentangling this effect from the luminosity dependence of the TF scatter will be tricky. There are many more low mass Scs than Sas and we measure more intrinsic scatter at the low mass end of the TF relation, so the average Sc should have a larger deviation from the mean TF relation than the average Sa. Whether the causal reason for this larger scatter at the low mass end of the TF is the lower mass of the galaxies, or the increased number of later

types is beyond the scope of this paper, but provides an interesting question for further study.

5. COMPARISON WITH OTHER TF RELATIONS

The first calibration of the TF relation in NIR bands was done by Aaronson *et al.* (1979). They found a slope of approximately $b = -9.5$ (or $L \propto v^{3.8}$) in the H-band using samples of galaxies in the two nearby clusters, Virgo and Ursa Major. This result was similar to the naive expectation of $L \propto v^4$ which arises from a simple consideration of the dynamics of spiral disks and the assumption that M/L is constant (see Appendix C of Courteau et al. 2007 for a recent discussion of simple analytic predictions for the TF slope). Aaronson *et al.* (1979) also observed that the scatter was lower than in the B-band TF, paving the way for significant work using the NIR TF relation.

There has been quite a lot of work on deriving template TF relations in the NIR bands since this initial paper. Here we attempt to compare some of these derivations with what we find here. This comparison is not complete, and is biased towards recent calibrations of the NIR TF relations. As has been shown here (and in M06) both the slope and zeropoint of the TF relation vary with morphological types. If this dependence is not corrected for then samples with different morphological type distributions should show different TF relations. In particular cluster samples may be more dominated by earlier type spirals (so expected to have shallower TF slopes) than field samples. Also it is not yet common practice to correct for incompleteness bias when deriving TF relations. TF relations uncorrected for incompleteness bias should all be shallower than what we derive here (with no other differences in the sample make up) – how much shallower they are will depend on the degree of incompleteness in the sample. Then there are hints that the TF relation slope varies with galaxy luminosity meaning that samples with different distribution of galaxy luminosities may also give different TF relations. With all these different factors to worry about it's clearly over simplistic to compare different calibrations directly. Never-the-less we provide such a direct comparison in Table 3, with brief comments about the different sample make-ups. In the remainder of this section we discuss each calibration in more detail.

Tully & Pierce (2000) derive TF relations in the B, R, I-bands using samples of galaxies drawn from 5 nearby clusters (with distance calibrators for the zeropoint). In a companion paper Rothberg et al. (2000) used a similar sample to derive the K-band TF relation. These papers claim that using the inverse relation "nulls" any bias introduced by sample incompleteness (however as discussed in several places this is only true in the case that there is no covariance between luminosity and width errors which is difficult to achieve in practice because of inclination dependent corrections) They find in I-band (for 155 galaxies) $M_I = -21.57 - 8.11(\log W - 2.5)$, while in K-band ($N = 65$) they find $M_K = -23.17 - 8.78(\log W - 2.5)$. This I-band relation is steeper than the bias corrected relation of M06 ($N = 807$), although consistent with M06's inverse fit with no incompleteness bias correction of $M_I - 5\log h = -20.89 - 8.341(\log W - 2.5)$. Rothberg et al. (2000)'s K-band relation is much shallower than both our preferred K-band result and our inverse fit to the sam-

ple with no incompleteness bias correction applied of $M_K - 5\log h = -22.250 - 10.005(\log W - 2.5)$, which could be due to the relatively small K-band sample size or the effects of incompleteness. This relation is similar to our fit to Sb galaxies, so the difference could also be explained if the Rothberg et al. (2000) sample is dominated by Sb and earlier type spirals. However this is not the case – this sample actually has almost equal numbers of Sb and Sc galaxies (see their Table 1).

Verheijen (2001) derive B, R, I and K-band templates for a sample of galaxies in the Ursa Major cluster. They claim this sample ($N = 16$) is complete. They find $M_I = -21.51 \pm 0.83 - (9.6 \pm 0.4)(\log W - 2.5)$ and $M_K = -23.05 \pm 0.95 - (10.6 \pm 0.4)(\log W - 2.5)$. The K-band relation is very similar to that found in this paper. The I-band relation is much steeper than that found in M06 and G97b.

Macri (2001) provides a Cepheid calibration of the H and K-band TF templates using 19 galaxies with Cepheid distances, for the 20th magnitude per arcsecond squared isophotal magnitudes in 2MASS they find $M_K = -22.34 \pm 0.07 - 10.4 \pm 0.5(\log W - 2.5)$ and $M_H = -22.01 \pm 0.02 - 10.5 \pm 0.4(\log W - 2.5)$. As must be the case for a sample based on galaxies with primary distances the sample size is small, and since galaxies with Cepheid distances tend to lie preferentially at the high mass end of the TF relation usually it's not a good idea to derive a slope from such a sample. The Macri (2001) K-band slope agrees with our result quite well, while the H-band slope is somewhat steeper.

Karachentsev et al. (2002) derive B, I, J, H and K TF relations for the most edge-on spirals in 2MASS. The 436 galaxies used are field spirals (therefore likely dominated by late type spirals) and are placed on the TF relation using absolute magnitudes derived with no correction for peculiar velocities. This could bias the slope as the impact of peculiar velocities is likely to be larger for galaxies at the low width end of the relation since they are more likely to be nearby. There is also no attempt to correct for sample selection biases. Only the slopes are reported: in the NIR they find $s_I = -6.37 \pm 0.18$, $s_J = -8.20 \pm 0.24$, $s_H = -8.71 \pm 0.25$, $s_K = -9.02 \pm 0.25$, shallower than we find in our bias corrected work as should be expected.

Theureau et al. (2007) use the "unbiased plateau" of field galaxies (as described in Theureau *et al.* 1998) to derive TF relations in the 2MASS J, H and K-bands. This method is iterative in that an input TF is used to derive distances to the galaxies from which an unbiased subset is used to construct a new input TF... and so on. They find (converted to the terminology used in this paper), $M_K = -23.5 - 6.6(\log W - 2.5)$, with $\sigma = 0.45$; $N = 990$, $M_H = -23.2 - 6.4(\log W - 2.5)$, with $\sigma = 0.47$, $N = 1166$ and $M_J = -22.7 - 6.3(\log W - 2.5)$, with $\sigma = 0.46$, $N = 960$. A Hubble's constant of $H_\circ = 57$ km s^{-1} Mpc^{-1} is implicit in these zeropoints. We correct to $H_\circ = 74$ km s^{-1} Mpc^{-1} for comparison with other work (see Table 3). The slopes of these relations are significantly shallower than we find in this paper for our Sc sample (and that are reported elsewhere in the literature). A possible explanation is that the difference is related to the luminosity distribution of the sample, in that the sample of Theureau et al. (2007) acts like a volume limited sample and is therefore dom-
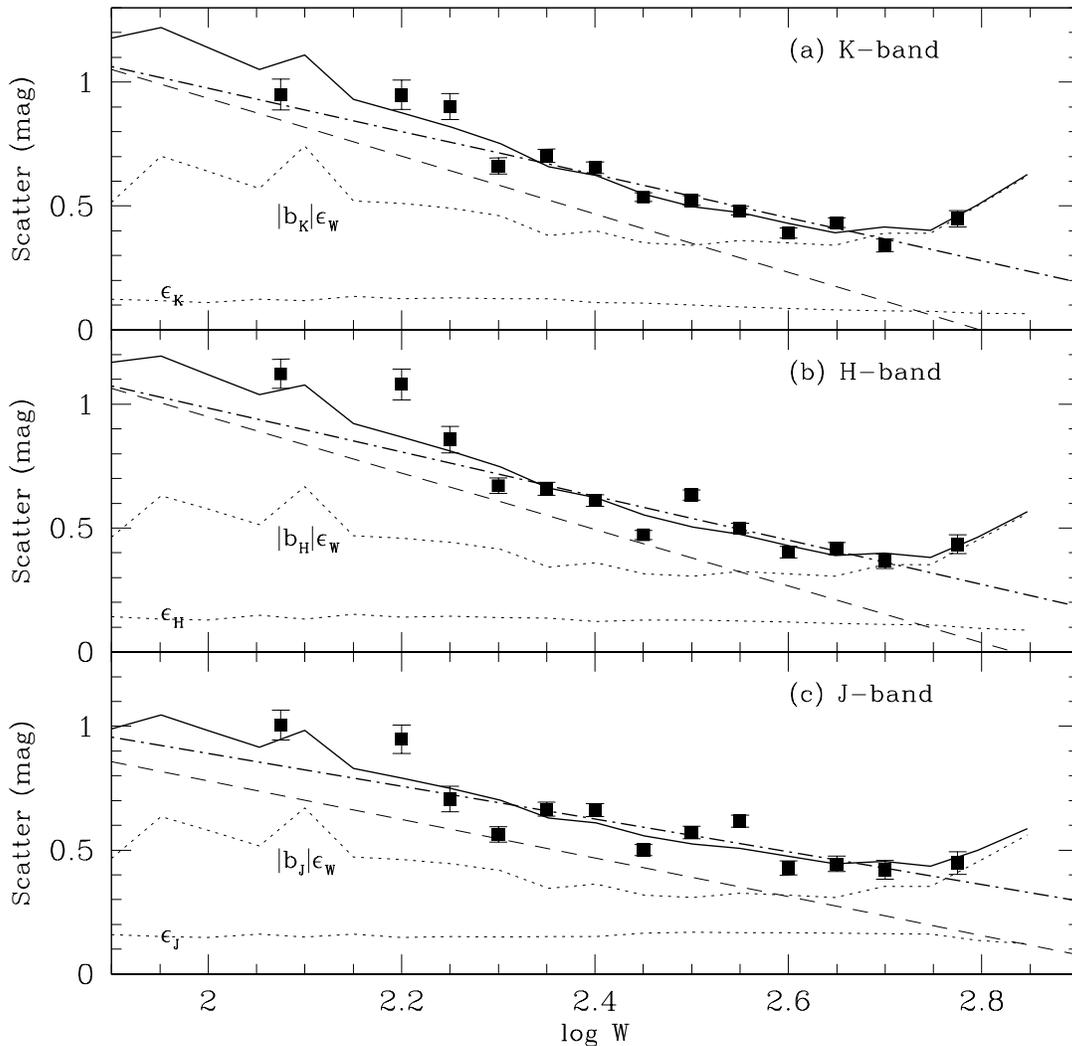
FIG. 5.— Total observed scatter in the TF relations in (a) K-band, (b) H-band and (c) J-band. The dash-dot line shows a linear fit to the total scatter. Also plotted is the error budget for all galaxies in the dataset as a function of rotation width. The dotted lines show errors associated with the photometry and width measurement (multiplied by the TF slope to be expressed in magnitudes). This is added in quadrature to a width dependent intrinsic scatter (shown by the dashed line – the sum is shown by the solid line) which is fit for.

inated by massive spirals, while the samples in this paper, in Verheijen (2001), Tully & Pierce (2000) and in Karachentsev et al. (2002) have many more low mass galaxies in them. If lower mass galaxies exhibit a steeper TF relation than massive spirals this could explain the difference between the measured slopes (Theureau 2007; priv. comm.). This idea is backed up to some extent by our investigation of the luminosity dependence of the slope, however these slopes are still significantly shallower than the direct fits to the most massive third of our sample suggesting that this cannot be the full explanation for the difference. Also Figure 9 of Theureau et al. (2007) shows that the sample to which the TF relation is fit in that paper does not differ significantly in $\log W$ extent from our sample (note that Theureau et al. 2007 use $\log V = \log W - \log 2 \sim \log W - 0.3$), so it does not seem likely that this can explain the large difference in TF slope. What appears to be a more likely explanation for

the difference in the slopes is the morphological make-up of the sample. A field sample like that in Theureau et al. (2007) might be expected to be dominated by the latest type spirals, however the selection of only the brightest field galaxies should instead bias it to earlier types. In fact the Theureau et al. (2007) sample (or at least the galaxies with new HI observations listed in their Table 3) is composed of more than half (64 %) Sab and earlier types ($T \leq 2$), and only 19% Sbs, and 17% Scs and later types. Comparing the slopes they find with our "Sa" TF relation the agreement becomes reasonably good.

Courteau et al. (2007) derive I- and K-band TF relations from a large dataset of both field and cluster spirals constructed from the combination of 4 smaller samples. In total they have 1303 galaxies which are placed on the I-band TF relation, only 360 of which ("the brightest SCII galaxies") are used to derive the K-band relation. They find (converted to the terminology used here, and to

TABLE 3
COMPARISION OF SOME PUBLISHED NIR TF RELATIONS.

Reference	I-band		J-band		H-band		K-band		Comments
	a	b	a	b	a	b	a	b	
This work			-21.65	-9.07	-22.49	-9.02	-22.68	-10.02	$N = 890$ (bias corrected, Sc)
This work			-21.67	-7.80	-22.50	-7.80	-22.69	-8.63	$N = 345$ (bias corrected, Sb)
This work			-21.87	-6.09	-22.65	-6.08	-22.80	-6.95	$N = 101$ (bias corrected, Sa)
(1)	-21.47	-8.59					-21.99	-9.29	$N_I = 1303$, $N_K = 360$
(2)			-22.1	-6.3	-22.6	-6.4	-22.9	-6.6	$N \sim 1000$ ("unbiased", 64% Sa)
(3)	-21.50	-7.85							$N = 807$ (bias corrected, Sc)
(3)	-21.38	-7.07							$N = 281$ (bias corrected, Sb)
(3)	-21.42	-5.52							$N = 61$ (bias corrected, Sa)
(4)		-6.37		-8.20		-8.71		-9.02	$N = 436$ (edge-on, field)
(5)	-21.51	-9.6					-23.05	-10.6	$N = 16$ (UMaj, complete?)
(6)					-22.01	-10.5	-22.34	-10.4	$N = 19$ (Cepheids)
(7)	-21.57	-8.11							$N = 155$ (cluster)
(8)							-23.17	-8.78	$N = 65$ (82 % Sb/Sc)
(9)	-21.01	-7.68							$N = 555$ (bias corrected, Sc)
(10)						-9.5			$N = 29$

NOTE. — Previous calibrations of the TF relation in I, J, H and K-bands are shown in order of publication date. Zeropoints are adjusted for $H_\circ = 74$ km s^{-1} Mpc^{-1} where necessary for comparison with those based on calibration from primary distances. References – (1) – Courteau et al. (2007), (2) Theureau et al. (2007), (3) – M06, (4) – Karachentsev et al. (2002), (5) – Verheijen (2001), (6) – Macri (2001), (7) – Tully & Pierce (2000), (8) – Rothberg et al. (2000), (9) G97b, (10) Aaronson *et al.* (1979).

$H_0 = 74$ km s^{-1} Mpc^{-1}) $M_I = -21.47 - 8.59(\log W - 2.5)$ and $M_K = -21.99 - 9.29(\log W - 2.5)$, fairly similar to the relations in M06 (for I-band) and found here (for K band). They also notice trends in the slope and zeropoint with both band and morphological type of the sample of the same sense we find in this paper (and was found in M06 for I-band) but of a smaller size. The slope of their Sc I-band TF relation ($N = 505$) is -9.19 mags/dex while for Sa's ($N = 117$) they find a slope of -8.25 mag/dex. In K-band they find for Sc's ($N = 166$) a slope of -9.80 mags/dex and for Sa's ($N = 56$) a slope of -9.12 mags/dex.

It is interesting to ask if our own Milky Way galaxy lies on the TF relation we find in this paper. A previous study by Malhotra et al. (1996) showed that the Milky Way was within 1.5σ of the NIR TF relations of other nearby galaxies. The availability of photometrically accurate all-sky surveys in these bands (like 2MASS and DIRBE) means that it is easier (although still difficult) to estimate the total luminosity of the Milky Way in these bands to place it on the TF relation. The total luminosity of the Milky Way was estimated in the J and K bands from DIRBE data by Malhotra et al. (1996) as $M_K = -24.06$ mags and $M_J = -23.05$ mags. Recent estimates of the total rotation velocity of the Milky Way vary between $v = 226 \pm 15$km s^{-1}(Lepine et al. 2008) and $v = 270$km s^{-1}(Méndez et al. 1999). We therefore use $W = 496 \pm 44$ km s^{-1}, or $\log W = 2.69 \pm 0.05$ to cover both ends of the estimate. The best guess of the morphological type of the Milky Way is that it is an Sc or SBc (Hodge 1983), meaning that it should lie on the Sc relations we derive above (see Equations 4) with no correction for morphology. We find that for $H_\circ = 74$ km s^{-1} Mpc^{-1}, the Milky Way is slightly underluminous, but consistent within the measured intrinsic scatter of both the J and K-band TF relations, being 0.32 mags dimmer than the J-band TF relation, and 0.53 mags dimmer than the K-band TF relation. If the larger rotational speed is accurate the deviation from the TF relations would be greater, using the small end of the rotation speed esti-

mates the Milky Way is entirely consistent with lying on the TF relation derived here.

6. SUMMARY AND DISCUSSION

The 2MASS Tully-Fisher Survey (2MTF) aims to measure Tully-Fisher (TF) distances to all bright inclined spirals in the 2MASS Redshift Survey (2MRS). Essential to this project is a universal calibration of the TF relation in the 2MASS J (1.2 μm), H (1.6 μm) and K (2.2 μm) bands. We present the first bias corrected (or universal) TF template in these bands. Previously published NIR TF relations have either ignored the issue of incompleteness bias affecting the slope and zeropoint derived, or have attempted to construct a complete sample from a cluster, or by using only part of their data.

As in earlier work, we find that the slope of the TF relation becomes steeper as the wavelength increases. We find that the slope is close to the simple theoretical expectation of $L \propto v^4$ in K-bands, while is is slightly shallower at H- and J-band at $L \propto v^{3.6}$. The change in zeropoint between bands in consistent with the mean colors of the galaxies in the template sample.

We investigate the dependence of the TF relation on galaxy morphology showing that in all three bands the relation is steeper for later type spirals which also have a dimmer TF zeropoint. We correct for this dependence in deriving a global TF relation for Sc galaxies in the NIR. We also investigate the luminosity dependence of the slope of the TF relation, finding hints that at both the highest and lowest masses the slope of the TF relation is shallower than the mean relation – however this effect is not large.

We fit the TF relation using direct, inverse and bivariate fits. We favor the bivariate fit which takes into account errors on both the width and magnitude measurements (we include the measured intrinsic scatter in the weighting of the fits) finding a TF template for Sc galaxies (but which can be applied to all spirals with a morphological correction) of:

$$M_K - 5\log h = -22.030 - 10.017(\log W - 2.5),$$

$$M_H - 5\log h = -21.833 - 9.016(\log W - 2.5), \quad (4)$$
$$M_J - 5\log h = -20.999 - 9.070(\log W - 2.5).$$

These relations are bases on 2MASS extrapolated magnitudes and rotation widths measured from the HI line of galaxies at the 50% level of the (peak$-rms$) on a fit to the edges of the profile (W_{F50}; supplemental widths from optical rotation curves are corrected to the W_{F50} scale using the prescription described in M06 based on work of Catinella *et al.* 2007). To measure a TF distance an observation of the inclination, i, of the galaxy is also required to correct the observed Doppler broadened width to the full rotational width of the galaxy, and to correct the observed total magnitude for extinction from dust internal to the galaxy. One would measure the distance to a galaxy using the deviation of a galaxy from this TF relation (ΔM) and its measured recessional velocity using

$$d = \frac{v_{\mathrm{CMB}}}{H_\circ} 10^{\frac{\Delta M}{5}}, \quad (5)$$

or (equivalently, but now independent of $H_\circ$) the peculiar velocity in the CMB frame is

$$v_{\mathrm{pec,CMB}} = v_{\mathrm{CMB}}(1 - 10^{\frac{\Delta M}{5}}). \quad (6)$$

Here $\Delta M = M_{\mathrm{obs}} - M(W)$ is the difference between $M_X(W) - 5\log h$ from the TF relations above (Equations 4, where $X = J, H$ or K describes the band the magnitude is measured in) and the corrected absolute magnitude of the galaxy, calculated from the observed apparent magnitude using

$$M_{\mathrm{corr}} - 5\log h = m_{\mathrm{obs}} - A_X - I_X + k_X - T_X - 5\log v_{\mathrm{CMB}} - 15. \quad (7)$$

The observed magnitude of a galaxy above, has a correction for extinction due to dust in our Galaxy (A_X), and internal to itself (I_X), as well as a cosmological K-correction (k_X). We use the prescription described in detail in Masters *et al.* (2003) to apply these corrections to the 2MASS extrapolated magnitudes. Also needed is a morphological type correction, $T_X(W)$ to correct for change in slope and zeropoint we see between different types of spirals. This correction depends on both the type, T and the rotational width of the galaxy and is described in Section 3 above. The observed width, W_{F50} must also be corrected for instrumental effects (Δ_s), inclination, cosmological broadening and the effect of turbulent motions (Δ_t) in the disk:

$$W_{\mathrm{corr}} = \left[\frac{W_{\mathrm{F50}} - \Delta_s}{1 + z} - \Delta_t\right] \frac{1}{\sin i}, \quad (8)$$

The instrumental correction will depend on the details of the telescope used see Springob *et al.* (2005) for more information on this. Based on arguments in Springob *et al.* (2005) we use $\Delta_t = 6.5$km s^{-1}.

The scatter in the TF relation is important to understand, both to properly derive distance/peculiar velocity errors derived from TF, and as a constraint to models of galaxy formation. We fit for an intrinsic TF scatter which varies with galaxy luminosity (following the methodology of G97b and M06). We find no evidence for significant variation of the scatter with the wavelength of the magnitudes used. We do observe that later type spirals on the mean have a larger intrinsic scatter than earlier types, however disentangling this effect from the luminosity dependence of the scatter is tricky (since there are more later types at the low mass end of the relation where the scatter is observed to be larger) and beyond the scope of this paper.

The TF relations derived in this paper will be used in future work to measure distances to galaxies in the 2MTF survey. The derivation of an unbiased or "universal" TF relation in the NIR J, H and K-bands should also be of significant use to constrain models of galaxy formation.

REFERENCES

Aaronson, M., Huchra, J. & Mould, J. 1979 ApJ 229, 1
Aaronson, M. & Mould, J. 1983 ApJ 265, 1
Catinella, B., Haynes, M. P., & Giovanelli, R. 2007, AJ, 134, 334
Catinella, B., Haynes, M.P. & Giovanelli, R. 2005, AJ, 130, 1037.
Courteau, S., Dutton, A. A., van den Bosch, F. C., MacArthur, L. A., Dekel, A., McIntosh, D. H., & Dale, D. A. 2007, ApJ, 671, 203
Cutri, R.M., Skrutskie, M.F., Van Dyk, S., Beichman, C.A., Carpenter, J.M., Chester, T., Cambresy, L., Evans, T., Fowler, J., Gizis, J., Howard, E., Huchra, J., Jarrett, T., Kopan, E.L., Kirkpatrick, J.D., Light, R.M, Marsh, K.A., McCallon, H., Schneider, S., Stiening, R., Sykes, M., Weinberg, M., Wheaton, W.A., Wheelock, S., Zacharias, N. 2006, *Explanatory Supplement to the 2MASS All Sky Data Release and Extended Mission Products*, http://www.ipac.caltech.edu/2mass/releases/allsky/doc/

Giovanelli, R., Haynes, M., Herter, T., Vogt, N.P., Wegner, G., Salzer, J.J., da Costa, L.N., & Freudling, W. 1997a, AJ, 113, 22.
Giovanelli, R., Haynes, M., Herter, T., Vogt, N.P., Wegner, G., Salzer, J.J., da Costa, L.N., & Freudling, W. 1997b, AJ, 113, 53 (G97b).
Haynes, M. P., Giovanelli, R., Salzer, J. J., Wegner, G., Freudling, W., da Costa, L. N., Herter, T., & Vogt, N. P. 1999a, AJ, 117, 1668
Hodge, P. W. 1983, PASP, 95, 721
Huchra, J. *et al.* 2005, in ASP Conf Proc., *Nearby Large-Scale Structures and the Zone of Avoidance*, ed. A. Fairall & P. Woudt (San Fransisco, CA: ASP)
Kannappan, S.J., Fabricant, D.G. & Franx, M. AJ, 123, 2358.
Karachentsev, I. D., Mitronova, S. N., Karachentseva, V. E., Kudrya, Y. N., & Jarrett, T. H. 2002, A&A, 396, 431

Kochanek, C. S., Pahre, M. A., Falco, E. E., Huchra, J. P.,
    Mader, J., Jarrett, T. H., Chester, T., Cutri, R. &Schneider, S.
    E. 2001, ApJ, 560, 566
Lepine, J. R. D., Dias, W. S., & Mishurov, Y. 2008, MNRAS (in
    press; astro-ph/0706.1811)
Macri, L.M. 2001, Ph.D. thesis, Harvard Univ.
Malhotra, S., Spergel, D. N., Rhoads, J. E., & Li, J. 1996, ApJ,
    473, 687
Masters, K.L. 2007, in ASP Conf. Proc. *Frontiers of
    Astrophysics: Celebration of NRAO 50th Anniversary Science
    Symposium* ed. A. Bridle, J. Condon and G. Hunt (San
    Fransisco, CA: ASP; in press; astro-ph/0708.2913)
Masters, K.L., Haynes, M.P., Giovanelli, R. & Springob, C.M.
    2006, ApJ, 653, 861; M06.
Masters, K.L. 2005, Ph.D. thesis, Cornell Univ.
Masters, K.L., Giovanelli, R. & Haynes, M.P. 2003, AJ, 126, 158.
Méndez, R. A., Platais, I., Girard, T. M., Kozhurina-Platais, V.,
    & van Altena, W. F. 1999, ApJ, 524, L39
Noordermeer & Verheijen 2007 MNRAS, 381, 1463
Peletier, R. F., & Willner, S. P. 1993, ApJ, 418, 626

Pierini, D. 1999, A&A, 352, 49
Pizagno, J., et al. 2007, AJ, 134, 945
Rothberg, B., Saunders, W., Tully, R. B., & Witchalls, P. L. 2000,
    ApJ, 533, 781
Sánchez, A.G., Baugh, C.M., Percival, W.J., Peacock, J.A.,
    Padilla, N.D., Cole, S., Frenk, C.S., & Norberg, P. 2006
    MNRAS, 366, 189
Schlegel, D. J., Finkbeiner, D. P., & Davis, M. 1998, AJ, 500, 525.
Springob, C.M., Masters, K.L. Haynes, M.H., Giovanelli, R. &
    Marinoni, C. 2007, ApJS, 172, 599.
Springob, C.M., Haynes, M.H., Giovanelli, R. & Kent, B. 2005,
    ApJS, 160, 149.
Theureau, G., Hanski, M. O., Coudreau, N., Hallet, N., & Martin,
    J.-M. 2007, A&A, 465, 71
Theureau, G., Rauzy, S., Bottinelli, L., & Gouguenheim, L. 1998,
    A&A, 340, 21
Tully, R.B. & Pierce, M.J. 2000, ApJ, 533, 744.
Verheijen, M. A. W. 2001, ApJ, 563, 694